

Microwave diagnostics of the position
of an acceleration site and pitch-angle
anisotropy of energetic electrons
in the flare 24 Aug 2002

*Melnikov, V.F.,
Reznikova, V.E., Shibasaki, K., Pyatakov
N.P., Myagkova I., Ji, H.*

Nobeyama Radioheliograph (野辺山電波太陽写真儀)



Discovery of looptop microwave sources in **optically thin part** of the frequency spectrum

Kundu et al 2001

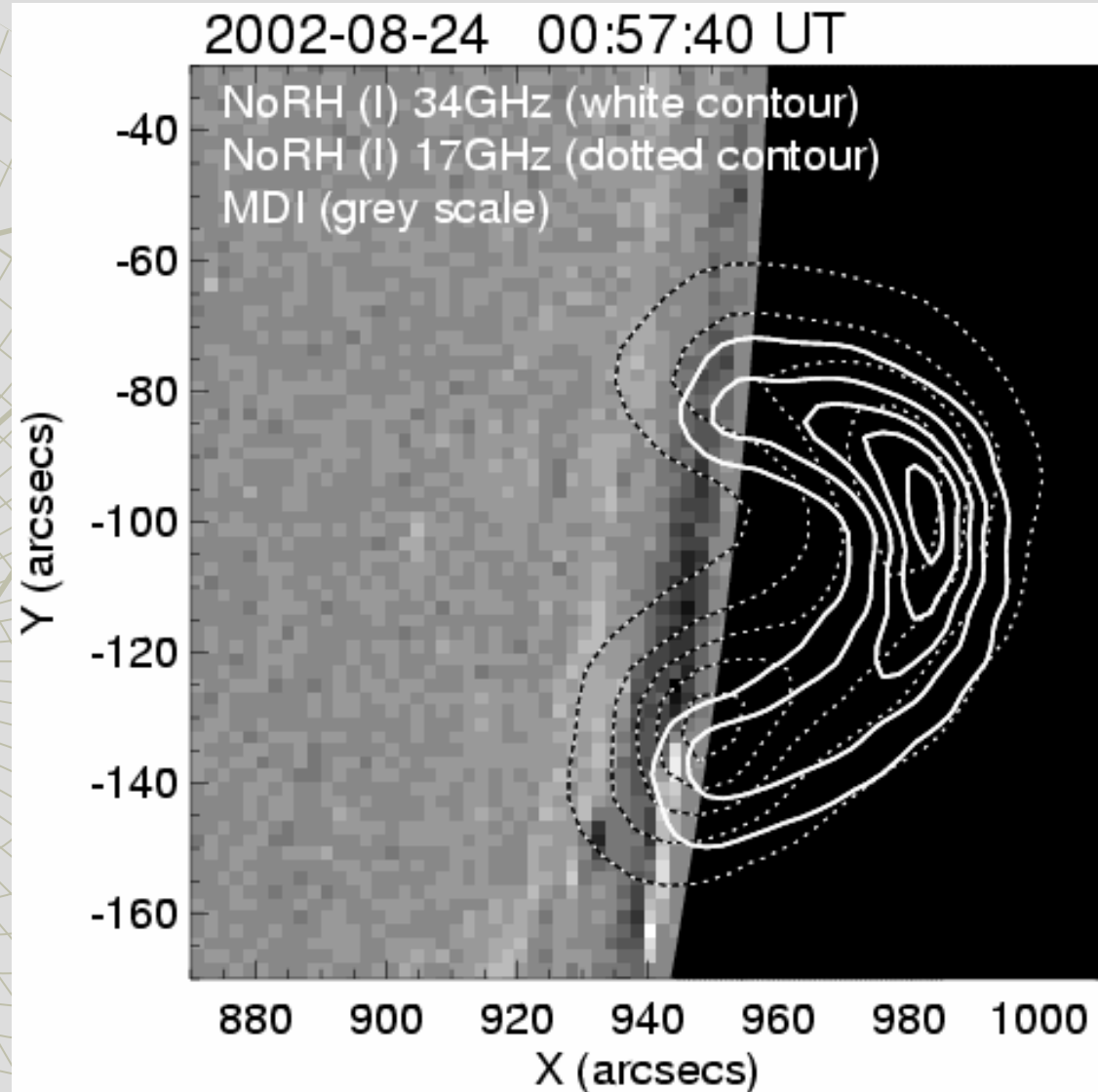
Melnikov et al 2002

Statistical results:

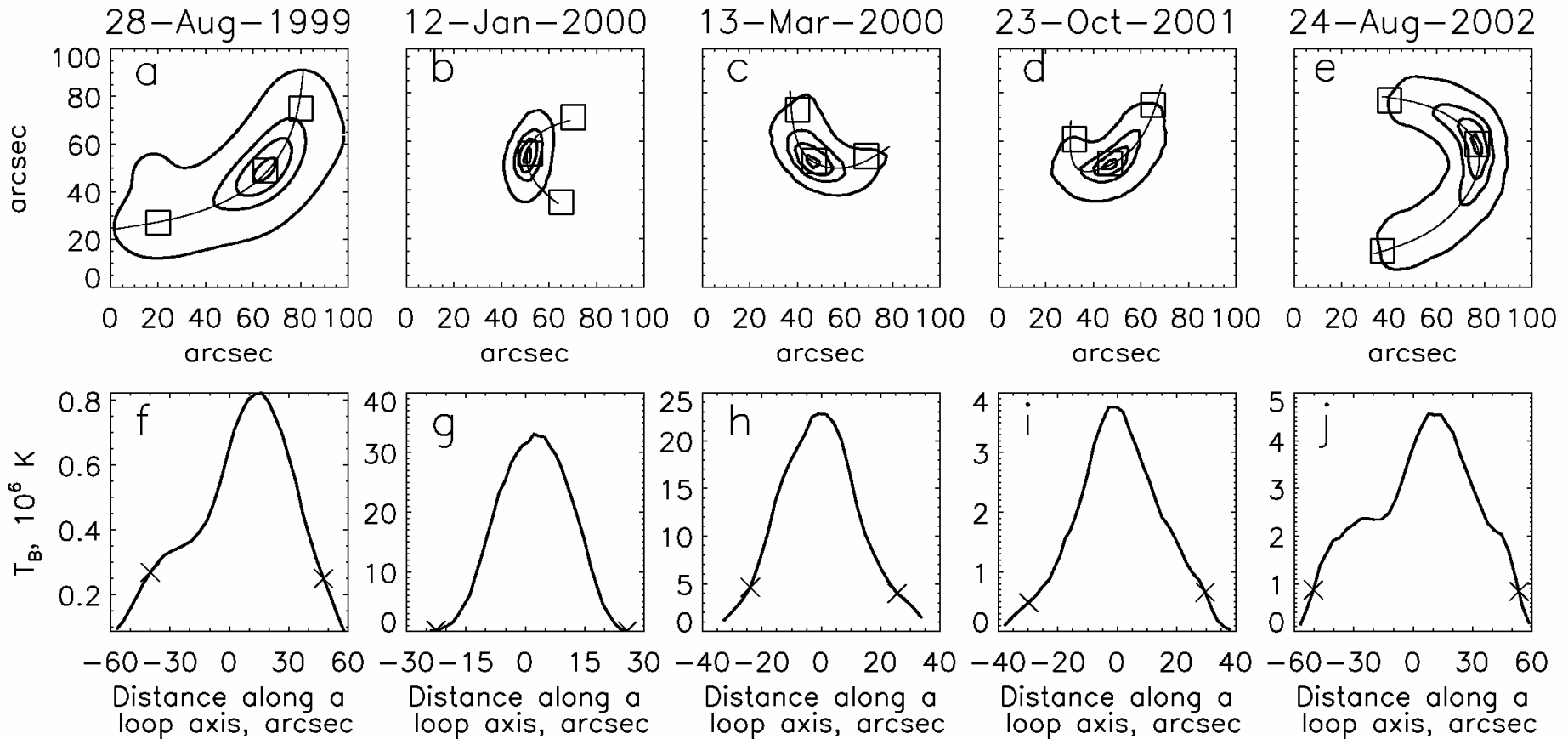
Martynova, Melnikov, Reznikova 2006

Tzatzakis, Nindos, Alissandrakis 2006

2009 г.



Spatial profiles of brightness at 34 GHz at the burst maximum



$$T_{bLT}/T_{bFP}: 3; 33; 6; 10; 6.$$

(Melnikov, Reznikova, Shibasaki, 2002, 2005)

Disagreement with the existing microwave loop models

The brightness peaks of optically thin GS emission have to be near the footpoints of extended loops with a nonuniform magnetic field as shown by *Alissandrakis and Preka-Papadema (1984)*, *Klein et al (1984)* due to strong dependence of GS intensity on the magnetic field strength.

For example, if the electron power law spectral index $\delta=4$, then

$$I_f \propto NB^{3.4} (\sin \theta)^{2.2}$$

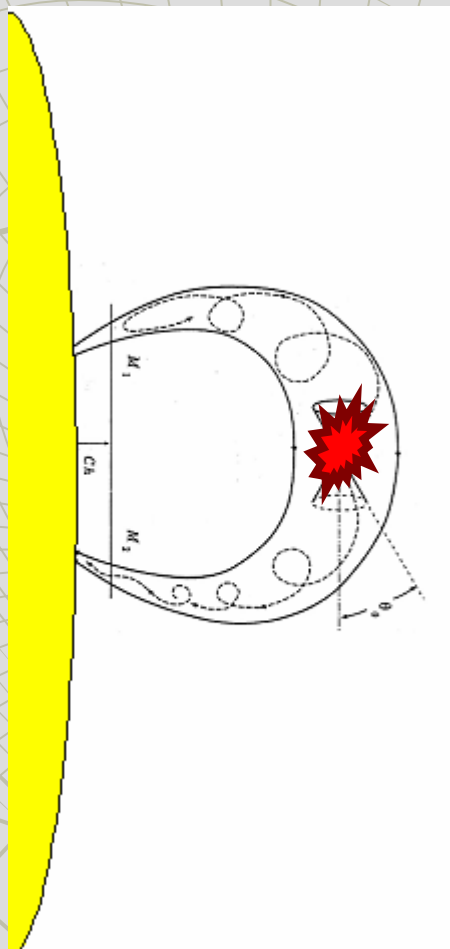
The possibility to have a hump in the brightness near the loop top due to the effect of optically thick emission (*Preka-Papadema & Alissandrakis 1992*, *Bastian et al 1998*) is ruled out in our case since for all the events under study the frequency spectral index between 17 and 34 GHz is negative and, therefore, the microwave emission from the loops is optically thin at least at 34 GHz.

What is the physical reason for the existence of microwave loop-top sources?

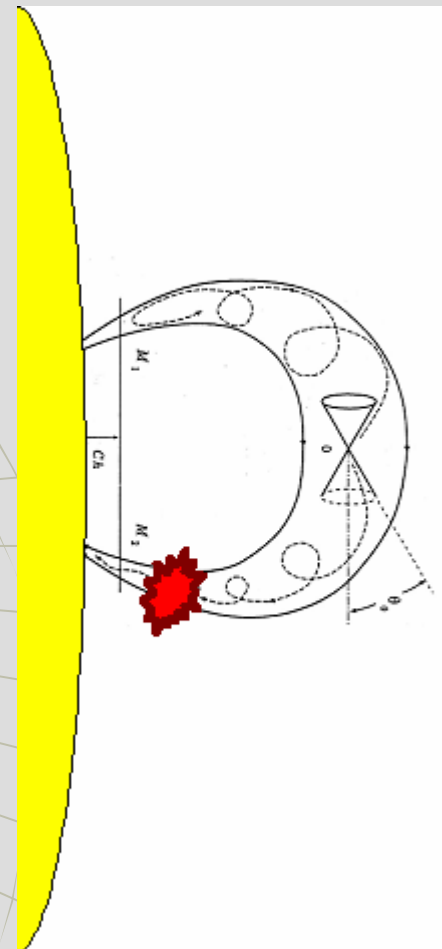
One of the most probable explanation of the loop-top source is a *strong concentration of mildly relativistic electrons in the upper part of a flaring loop*

Melnikov V.F., K. Shibasaki, V.E. Reznikova, 2002

Case 1

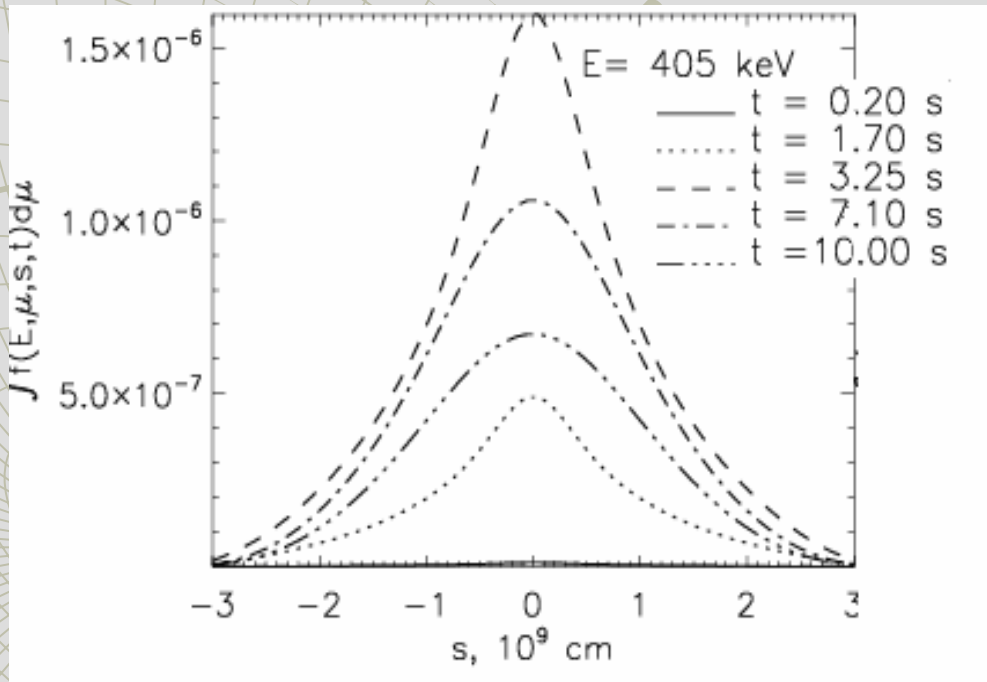


Case 2



Dynamics of the high energy electron distribution along a flaring loop

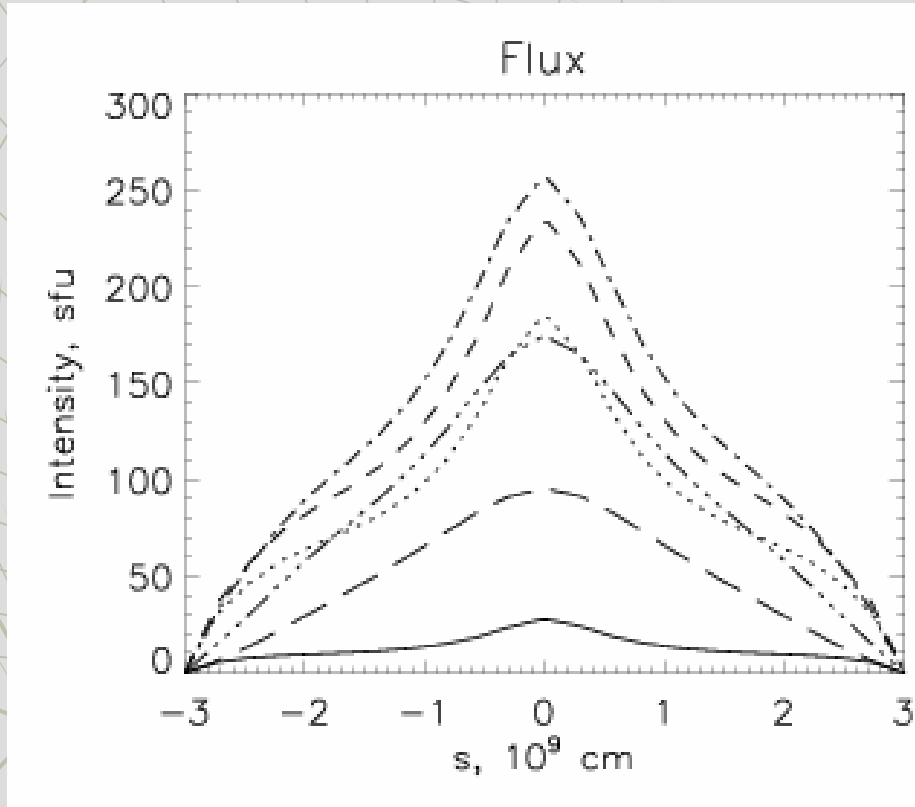
Case 1: Injection at the looptop



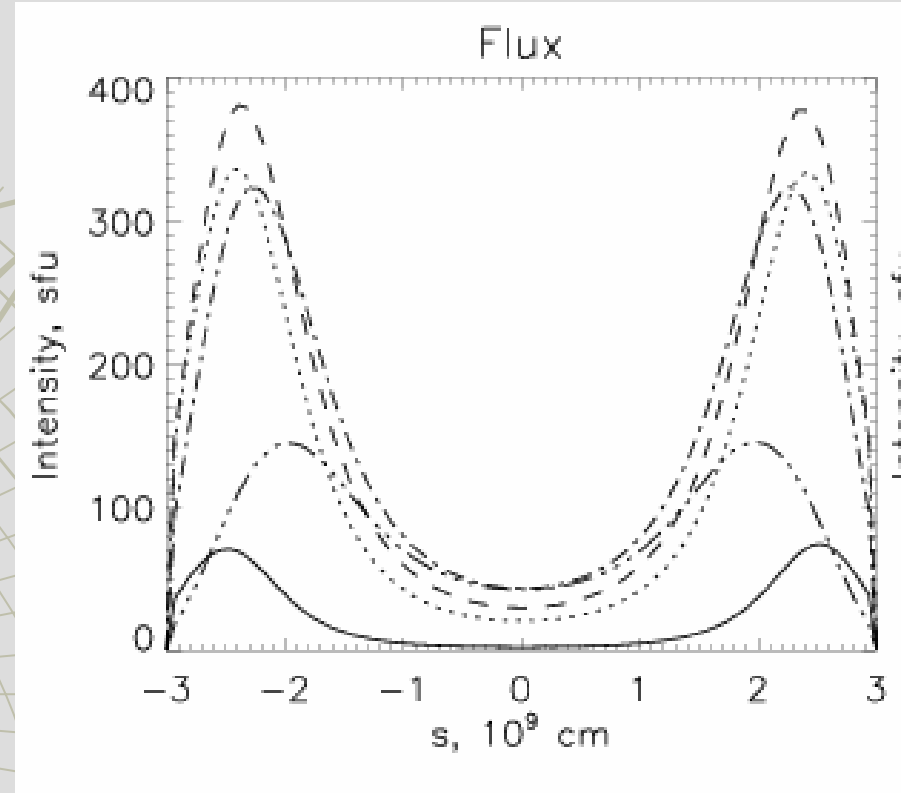
$s=0$ corresponds the loop center. Injection is isotropic. Mirror ratio $\kappa=5$. Plasma density $n_0=5 \cdot 10^{10} \text{ cm}^{-3}$ throughout the loop

Radio brightness distribution

Case 1: Injection at the loop top



Case 2: Injection near a footpoint

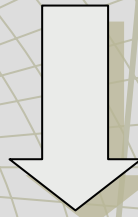


17 GHz

- $t = 10.00 \text{ s}$
- $t = 25.00 \text{ s}$
- - - $t = 30.00 \text{ s}$
- · - · $t = 40.00 \text{ s}$
- - - - $t = 60.00 \text{ s}$

Analysis of NoRH data showed that microwave brightness distribution along an extended flaring loops is not constant during the flare

- 1) *V.F. Melnikov, K. Shibasaki, V.E. Reznikova, APJ, 580, L185 (2002)*
- 2) *S.M. White, M.R. Kundu, V.I. Garaimov, T. Yokoyama, J. Sato, APJ., 576, 505 (2002)*
- 3) *O. V. Martynova, V.F. Melnikov, V.E. Reznikova (2007), : dynamics is observed in 80% of flares*



The next step:

to study the evolution of microwave brightness distribution along a loop, which may shed a light on the nonthermal electrons transport and acceleration site location in particular event.

A good example: the flare of 24 Aug 2002

GOES: X3.1

NOAA Number:

10069

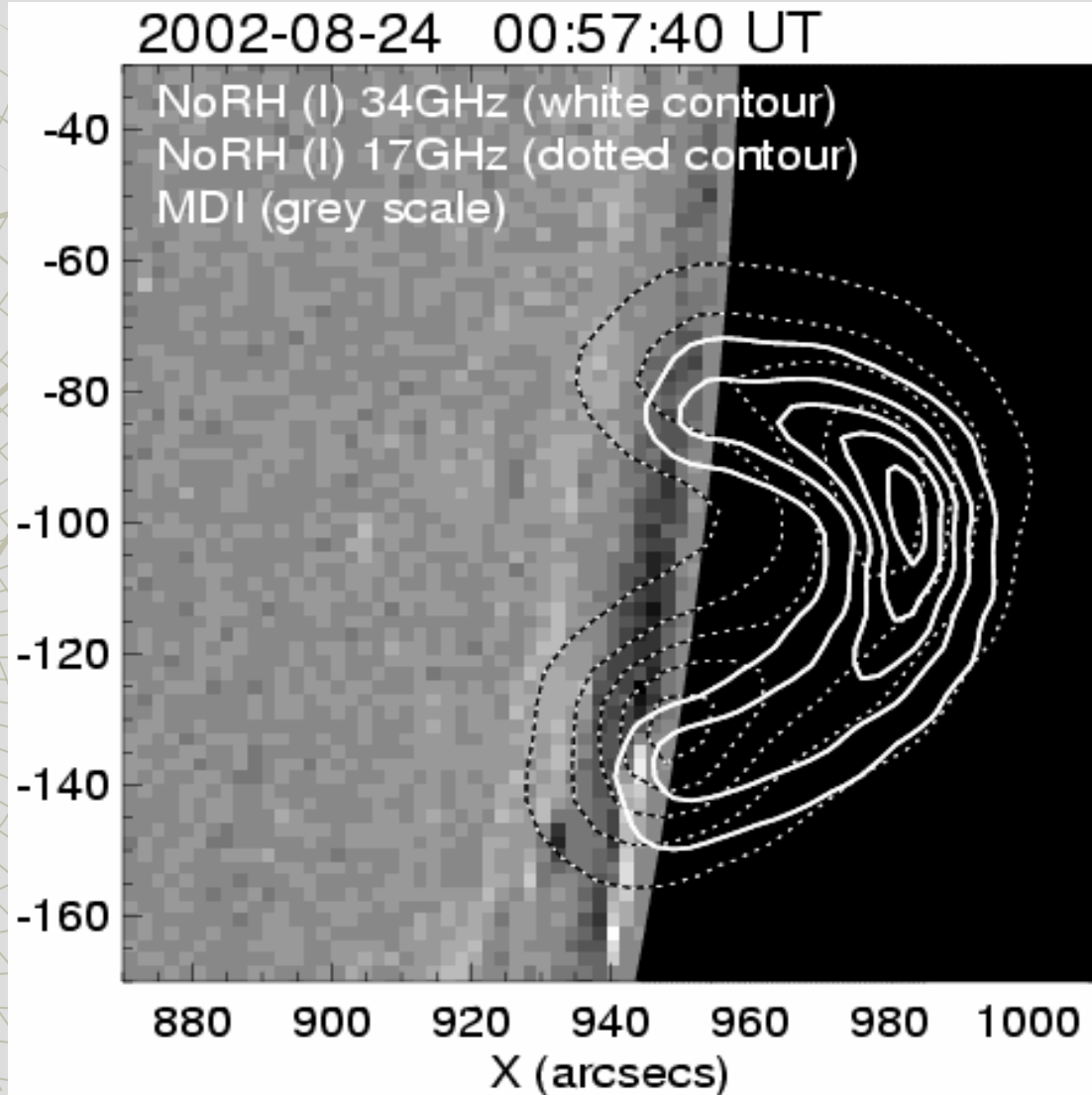
Position: S01W73

FP separation $\sim 5 \times 10^4$ km (70")

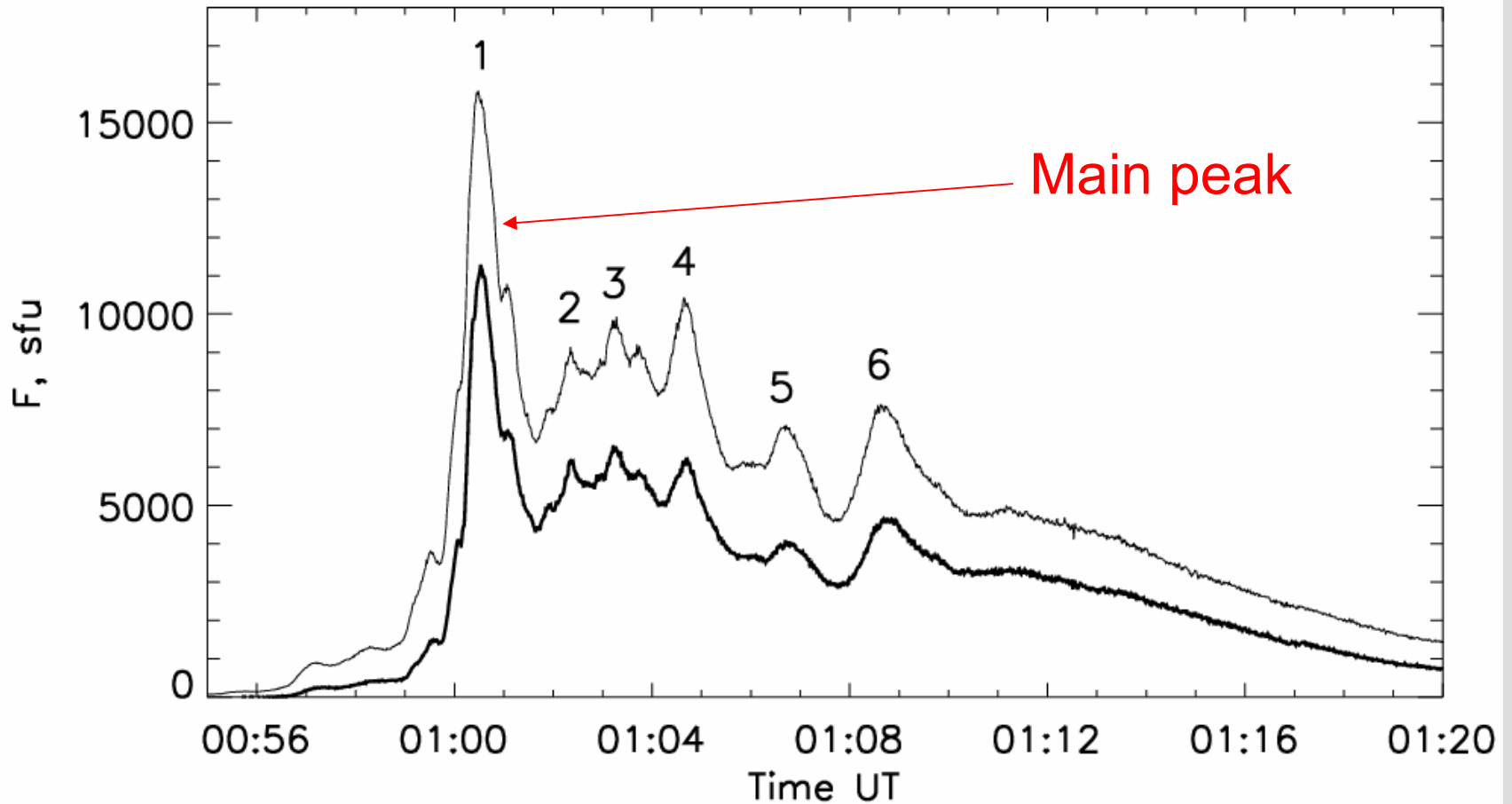
Max height $\sim 3.3 \times 10^4$ km (42")

(Reznikova et al ApJ 2009)

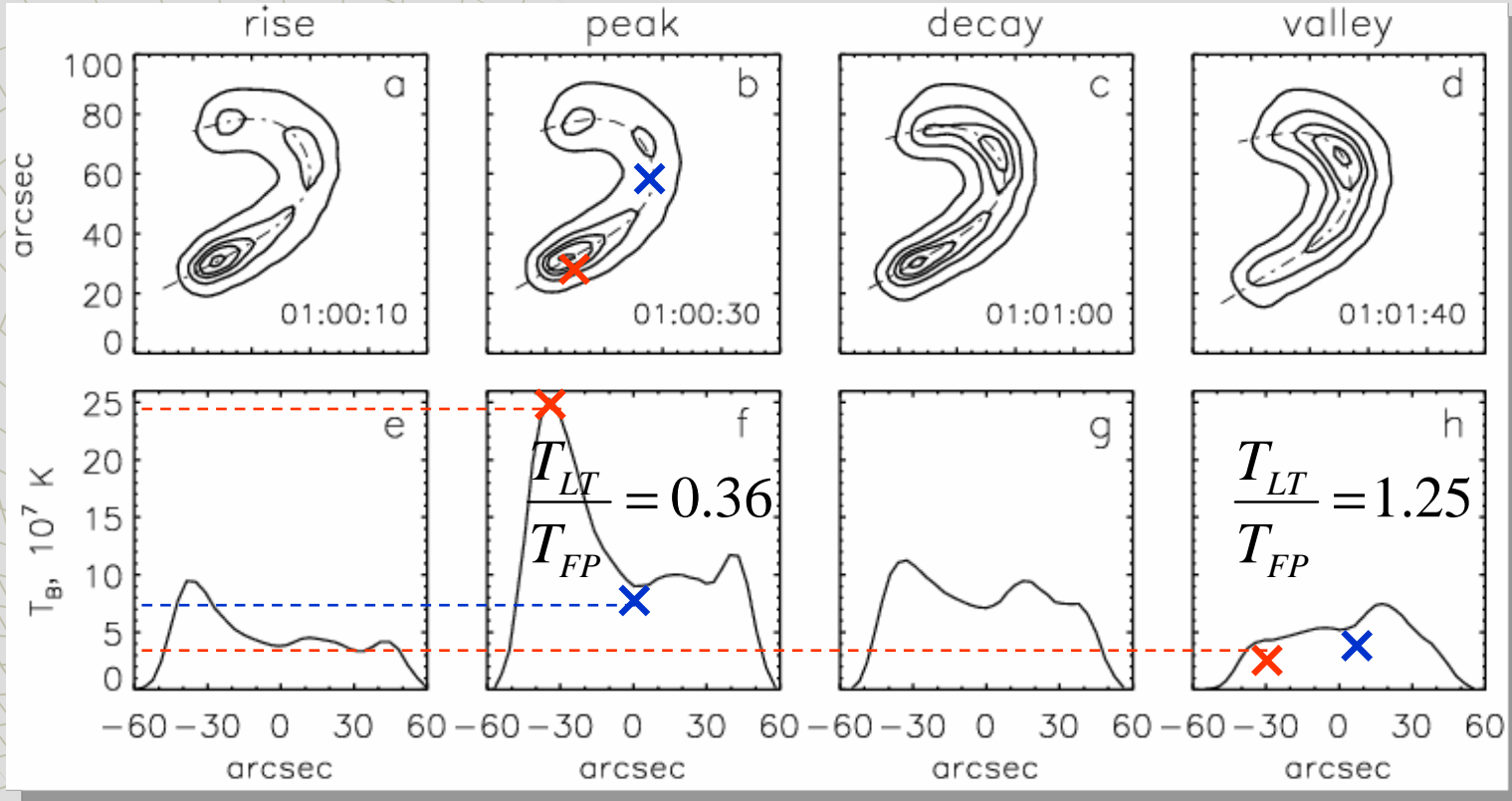
2009 г.



NoRP time profiles

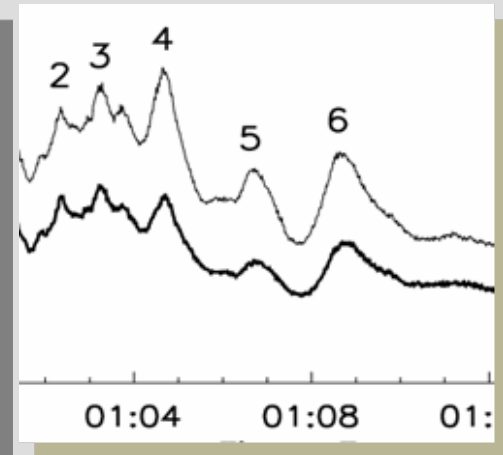
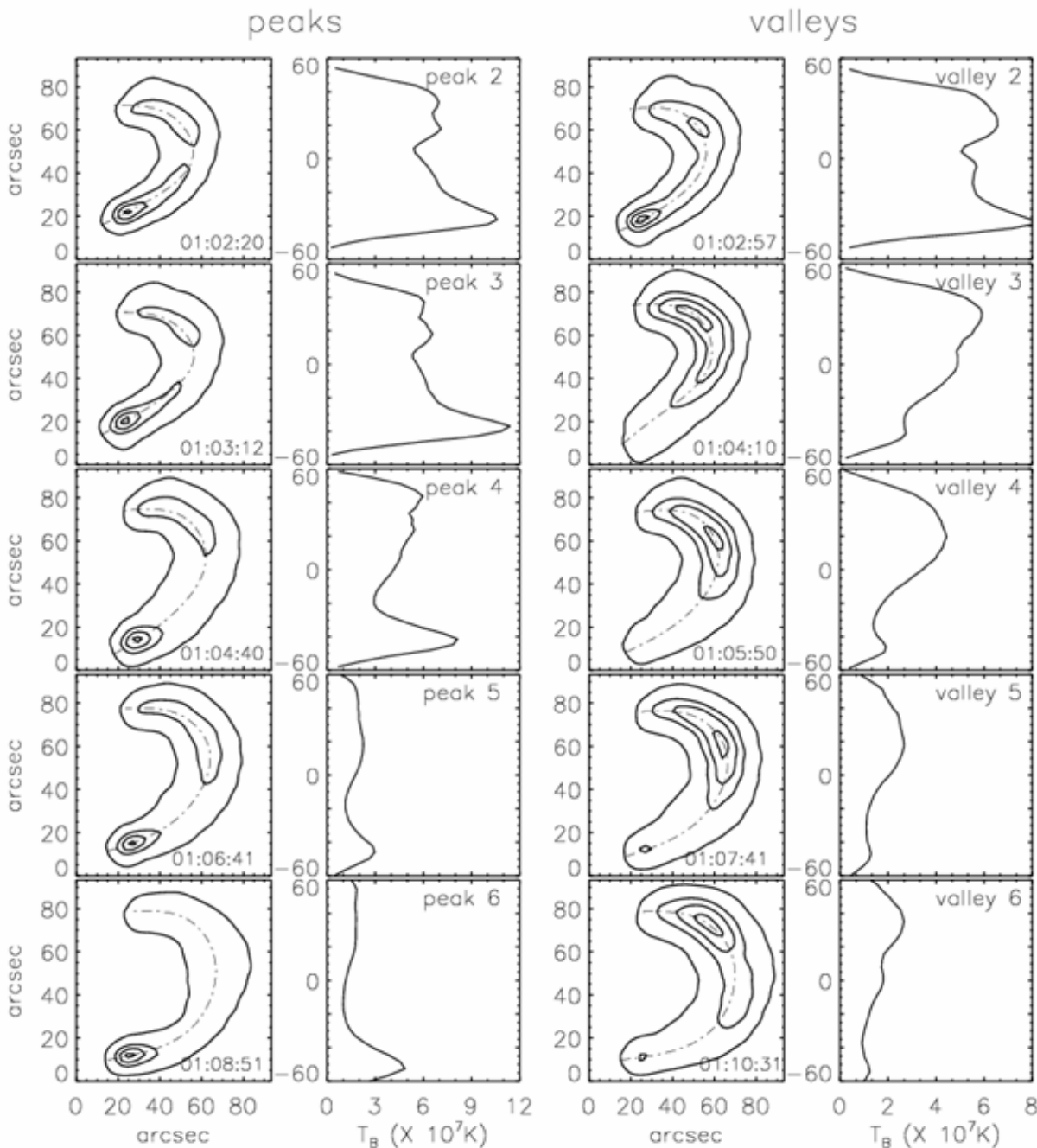


Main peak: Dynamics of brightness distribution at 34 GHz



Top panel: contour images of the radio source at four different moments

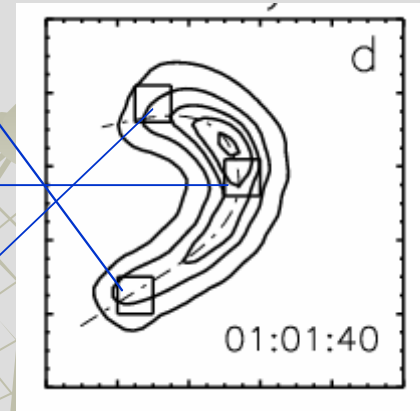
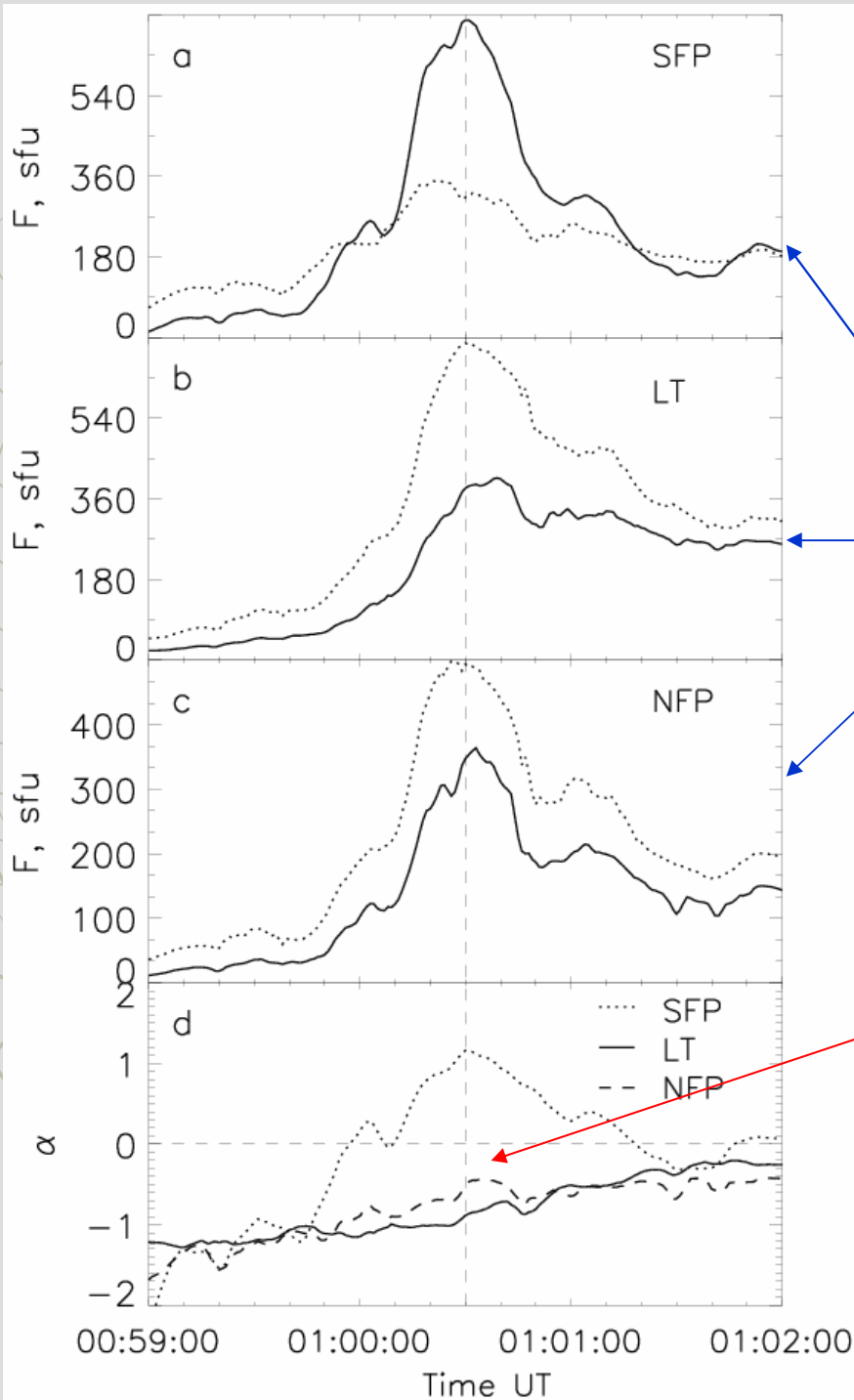
Bottom panel: spatial distributions of radio brightness temperature at 34 GHz along a visible flaring loop axes at the corresponding moment of time



The similar tendency in dynamics of radio emission distribution for all temporal sub-peaks!!

Every new injection of nonthermal electrons (rising and peak times) results in redistribution of brightness toward FPs. After injection maximum (decay ph.) emission gradually comes to localize in the upper section of the loop.

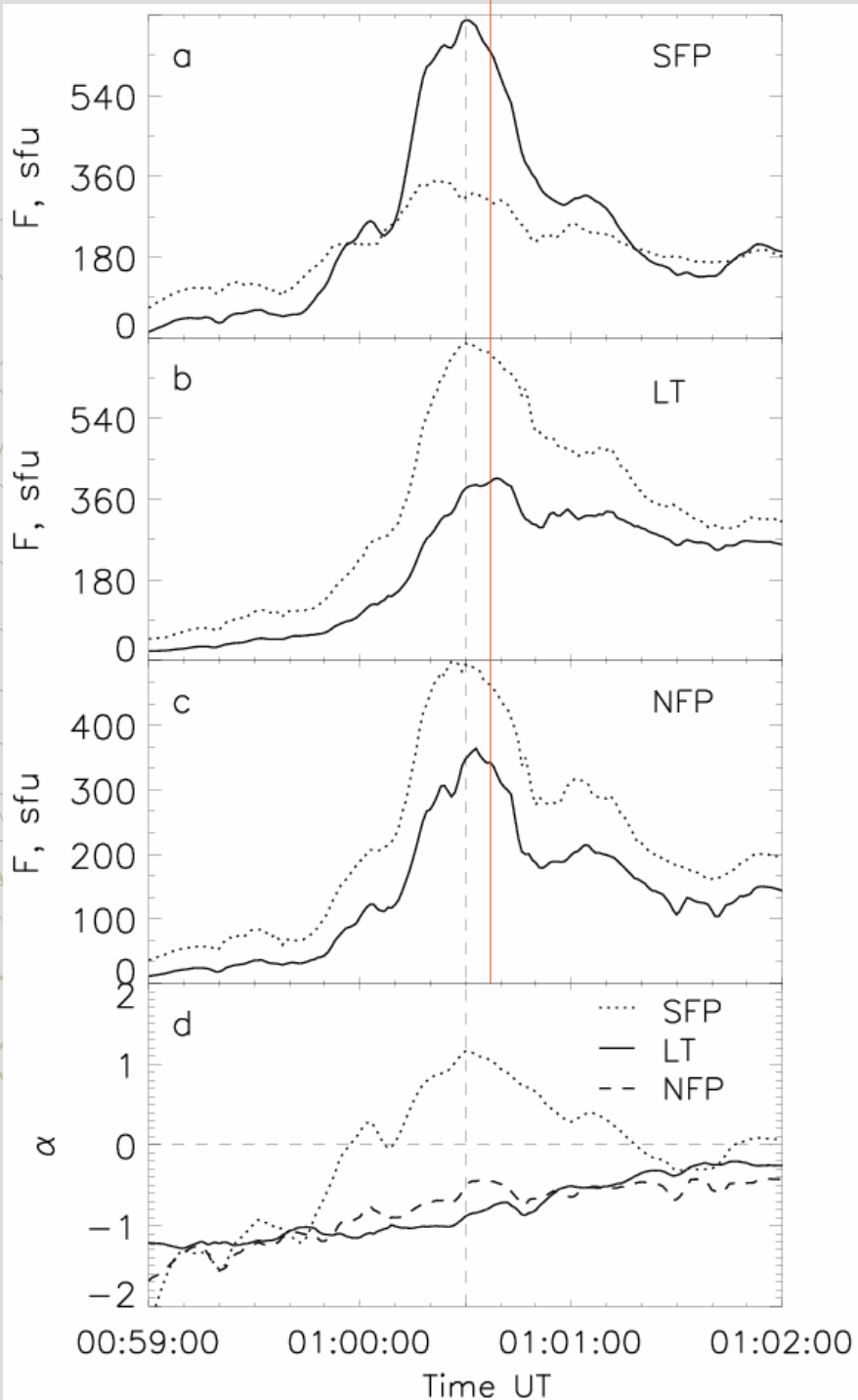
Comparative analysis of the emission time profiles generated in different parts of the loop (main peak)



SFP source is optically thick!
(see Melnikov, Gary and Nita, 2008)

$$\alpha = \ln (F_{34}/F_{17}) / \ln (34/17)$$

17 GHz (dotted lines)
34 GHz (solid lines)



Time delays:

- ❑ emission maxima from the LT are delayed against the maxima from the FP sources for both frequencies (4 ± 1 s for NFP & 8 ± 1 s SFP at 17GHz)
- ❑ delays are more pronounced at 34GHz (6 ± 1 s for NFP & 9 ± 1 s SFP)
- ❑ delay of the burst emission at higher frequency, 34 GHz, against that at 17 GHz

Spectral index:

- ✓ α is negative for the LT & NFP => optically thin at least at 34GHz
- ✓ α is positive for SFP => optically thick emitting GS source at 17 GHz

HXR- and gamma-ray emission of the flare

- ✓ **No RHESSI data for the impulsive phase**
- ✓ **Spectrometer **SONG** aboard of space solar observatory **CORONAS-F****

- **Launched July 31, 2001**

<http://coronas.izmiran.ru>



HX-ray spectral index



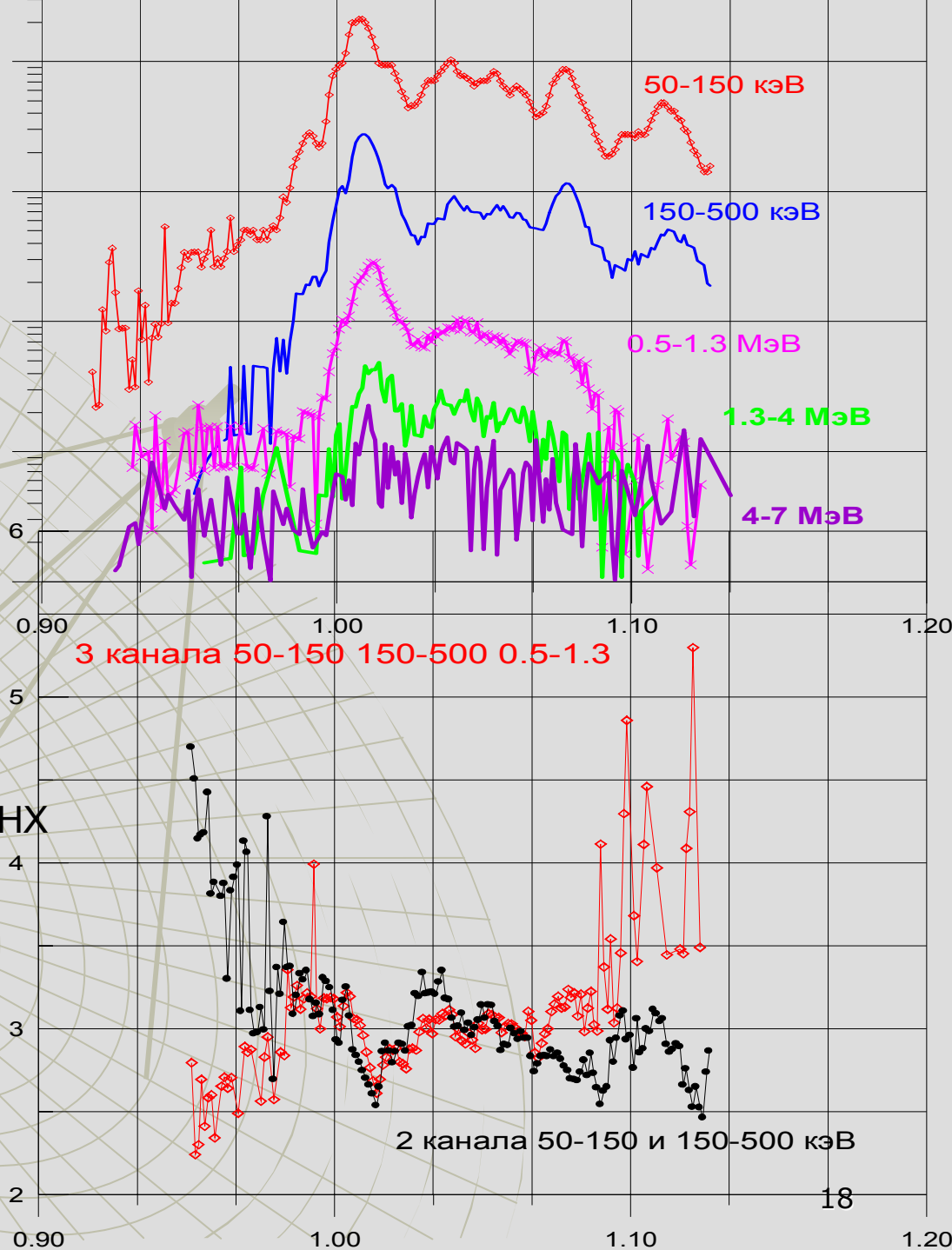
electron spectral index

$$\delta_e = \delta_{HX} + 1$$

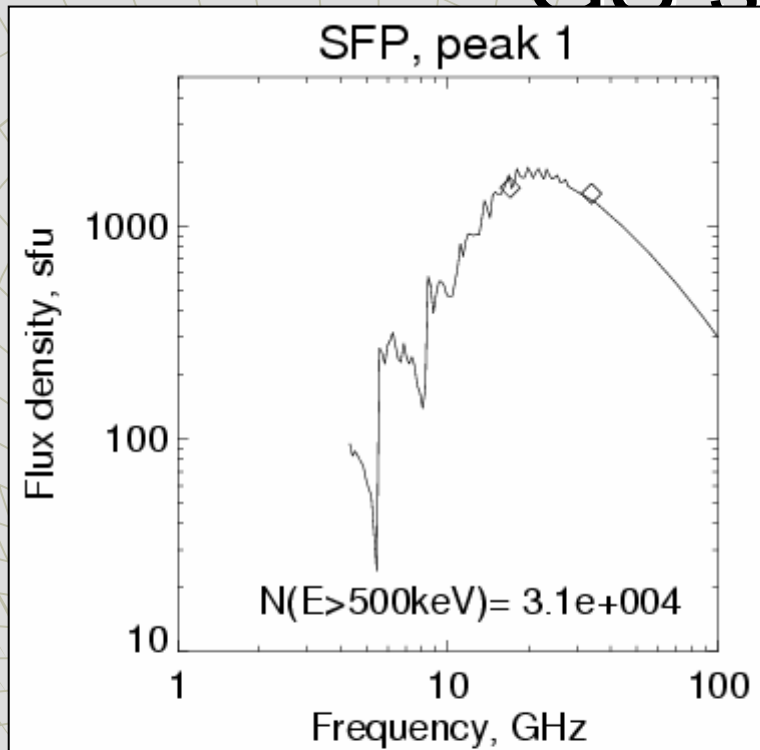
Peak 1: $\delta_{HX} = 2.6$ $\delta_e = 3.6$

Valley 1: $\delta_{HX} = 3.1$ $\delta_e = 4.1$

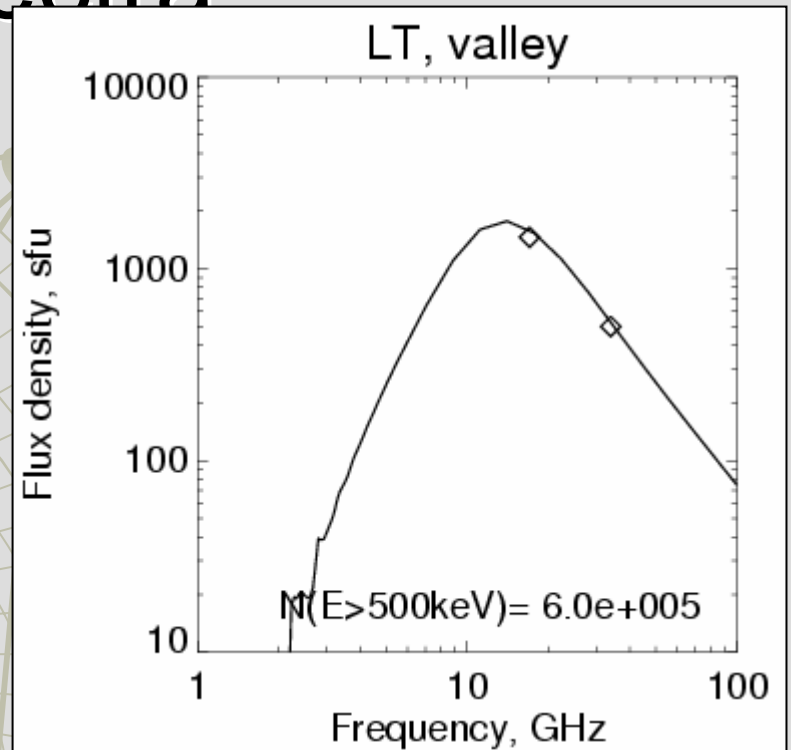
2009 г.



Estimation of accelerated electrons number density by approximation of GS spectra



$\delta_1 = 2.1$ $\delta_2 = 3.6$ $E_{12} =$
 $N(E>1\text{ MeV}) = 8.4\text{e}+003$
 $B = 1000.0\text{ G}$
 $n_0 = 8.0\text{e}+010\text{ cm}^{-3}$
Source depth = $1.6\text{e}+008$



$\delta_1 = 2.6$ $\delta_2 = 4.1$
 $N(E>1\text{ MeV}) = 1.2\text{e}+005$
 $B = 200.0\text{ G}$
 $n_0 = 4.0\text{e}+010\text{ cm}^{-3}$
Source depth = $3.6\text{e}+008$

Diagnostics of B and N in the LT & SFP sources

SFP source is optically thick at 17 GHz! $B_{SFP} \sim 1000 \text{ G}$

$$B_{LT} \sim 200 \text{ G}$$

- ◆ at peak 1: $N_{LT}(>500\text{keV}) = 9 \times 10^5 \text{ cm}^{-3}$
 $N_{SFP}(>500\text{keV}) = 3 \times 10^4 \text{ cm}^{-3}$

$$N_{LT} = N_{SFP} \times 30$$

- ◆ at valley 1: $N_{LT}(>500\text{keV}) = 6 \times 10^5 \text{ cm}^{-3}$
 $N_{SFP}(>500\text{keV}) = 3 \times 10^3 \text{ cm}^{-3}$

N_{LT} / N_{SFP} has grown about 7 times

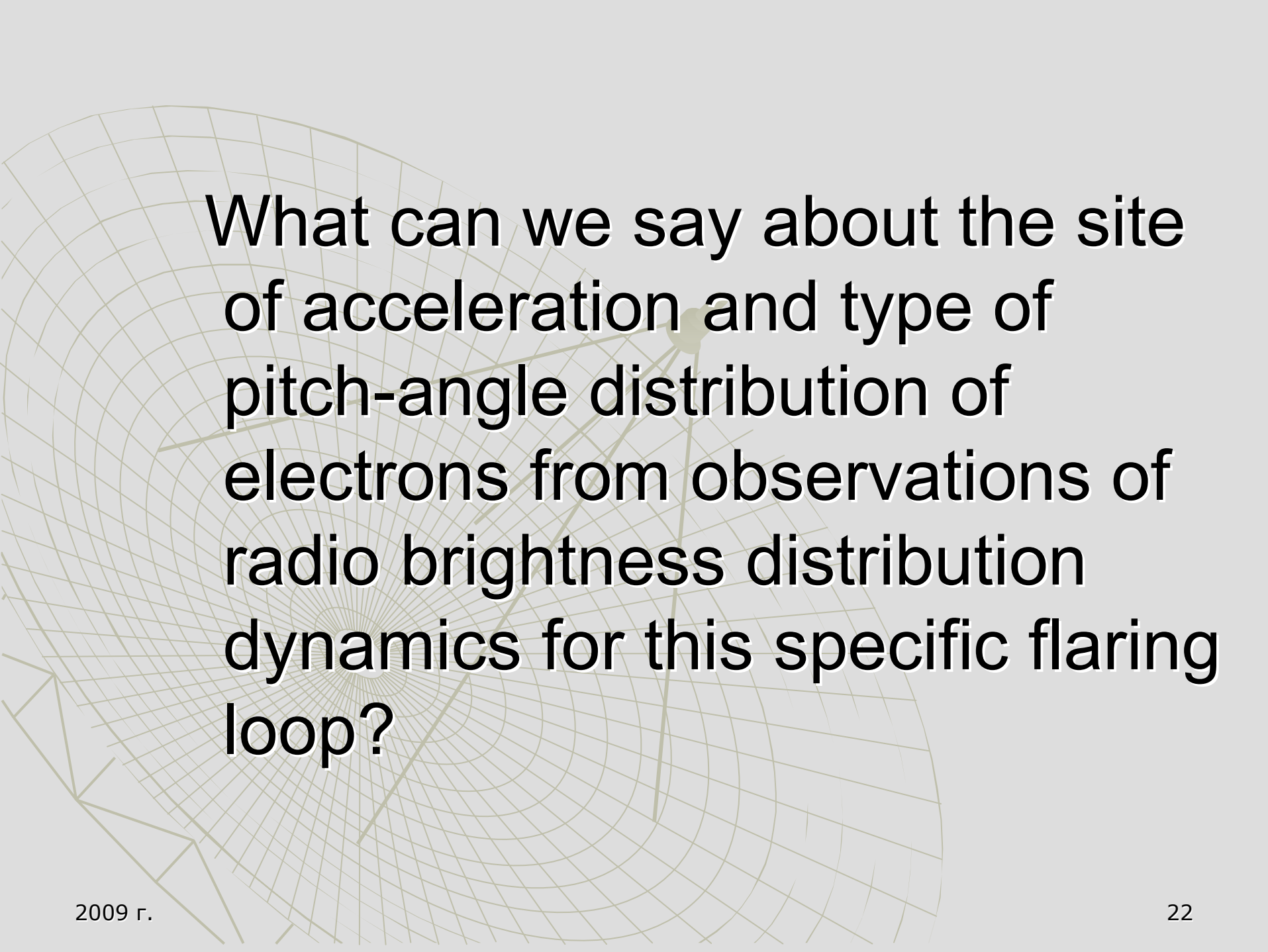
What is the physical reason for the dynamics of brightness distribution?

The most probable explanation:

strong relative increase of electron number density near the loop top, similar to the explanation proposed for the famous looptop optically thin microwave sources (Melnikov, Shibasaki, & Reznikova 2002)

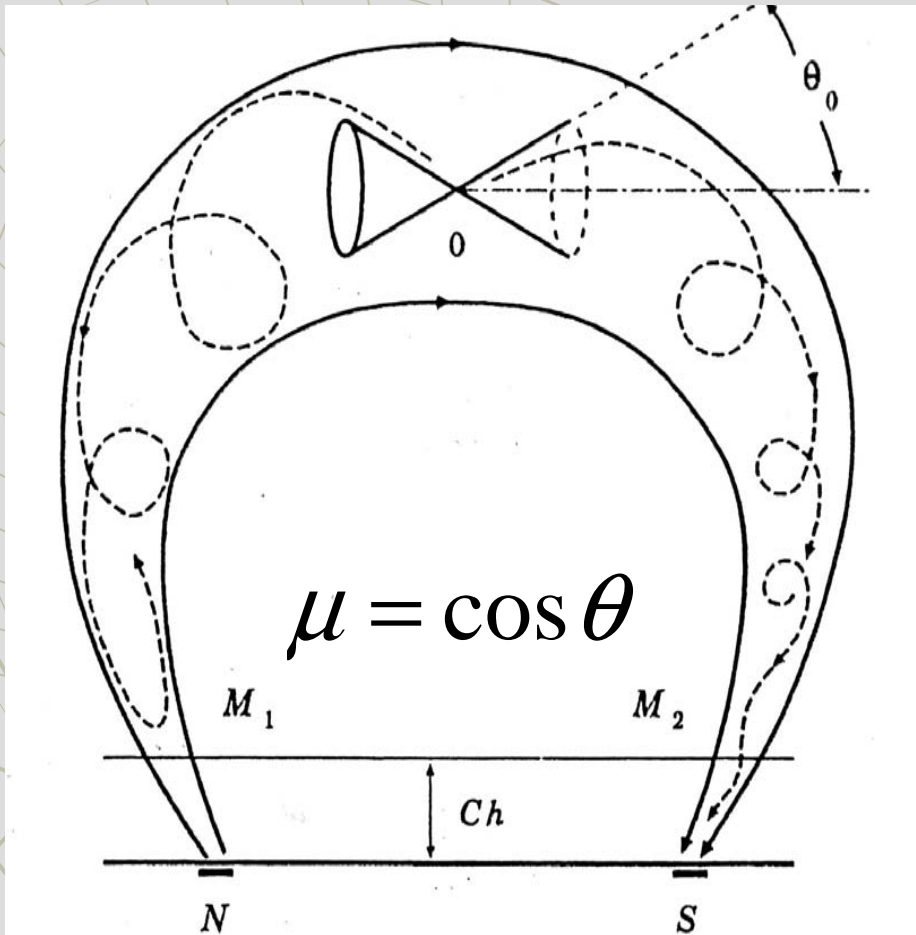
The reason is the influence of transport effects:

- 1) faster scattering of nonthermal electrons into a loss-cone in the lower part of the loop and, on the contrary,
 - 2) their better accumulation in its upper part (Melnikov 2006).
- The effects naturally act after each new electron injection resulting in the oscillatory re-distribution of brightness in the loop.



What can we say about the site of acceleration and type of pitch-angle distribution of electrons from observations of radio brightness distribution dynamics for this specific flaring loop?

Transport effects



What types of anisotropic distributions in different parts of a flaring magnetic loop are expected for various models of acceleration/injection?

The loss-cone condition:

$$\theta < \arcsin (B_s/B_m)$$

$$[1 - \mu^2(s)]/B(s) = \text{const.}$$

Dinamics of Nonthermal Electrons in Magnetic Loops

In a magnetic loop, a part of injected electrons are trapped due to magnetic mirroring and the other part directly precipitates into the loss-cone. The trapped electrons are scattered due to Coulomb collisions and loose their energy and precipitate into the loss-cone.

A real distribution strongly depends on the injection position in the loop and on the pitch-angle dependence of the injection function

$S(E, \mu, s, t)$, and also on time (Melnikov et al. 2006; Gorbikov and Melnikov 2007).

Non-stationary Fokker-Plank equation (Lu and Petrosian 1988):

$$\begin{aligned} \frac{\partial f}{\partial t} = & -c\beta\mu \frac{\partial f}{\partial s} + c\beta \frac{d \ln B}{ds} \frac{\partial}{\partial \mu} \left[\frac{1 - \mu^2}{2} f \right] + \frac{c}{\lambda_0} \frac{\partial}{\partial E} \left(\frac{f}{\beta} \right) + \\ & + \frac{c}{\lambda_0 \beta^3 \gamma^2} \frac{\partial}{\partial \mu} \left[(1 - \mu^2) \frac{\partial f}{\partial \mu} \right] + S(E, \mu, s, t) \end{aligned}$$

Initial and boundary conditions

Initial condition $f(E, \mu, s, 0) = 0$. (no electrons at moment $t = 0$)

Boundary condition, s $f(E, \mu > 0, s_{\min}, t) = 0$, $f(E, \mu < 0, s_{\max}, t) = 0$.

(precipitated electrons do not come back into the magnetic loop)

Injection function: $S(E, \mu, s, t) = S_1(E)S_2(\mu)S_3(s)S_4(t)$,

$$S_1(E) = (E / E_0)^{-\delta}$$

$$S_2(\mu) = \exp[-(\mu - \mu_1)^2 / \mu_0^2]$$

$$S_3(s) = \exp[-(s - s_1)^2 / s_0^2]$$

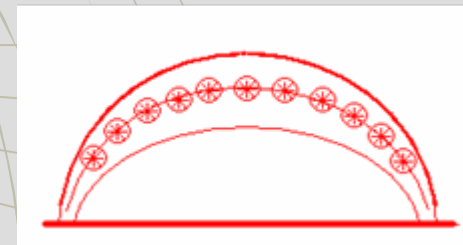
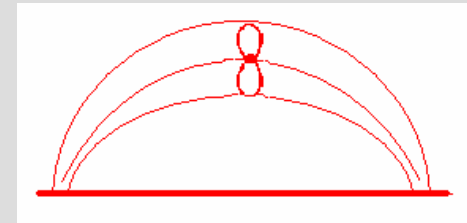
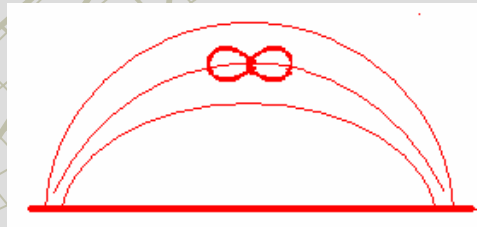
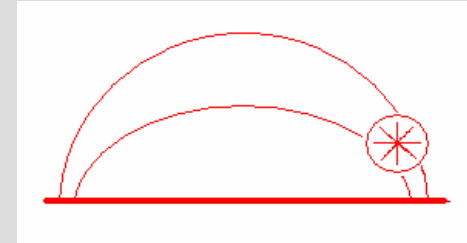
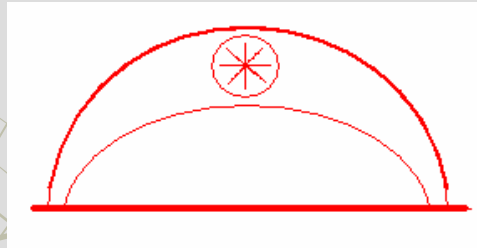
$$S_4(t) = \exp[-(t - t_1)^2 / t_0^2]$$

In the case of isotropic injection: $S_2(\mu) = \text{const}$

Numerical experiments

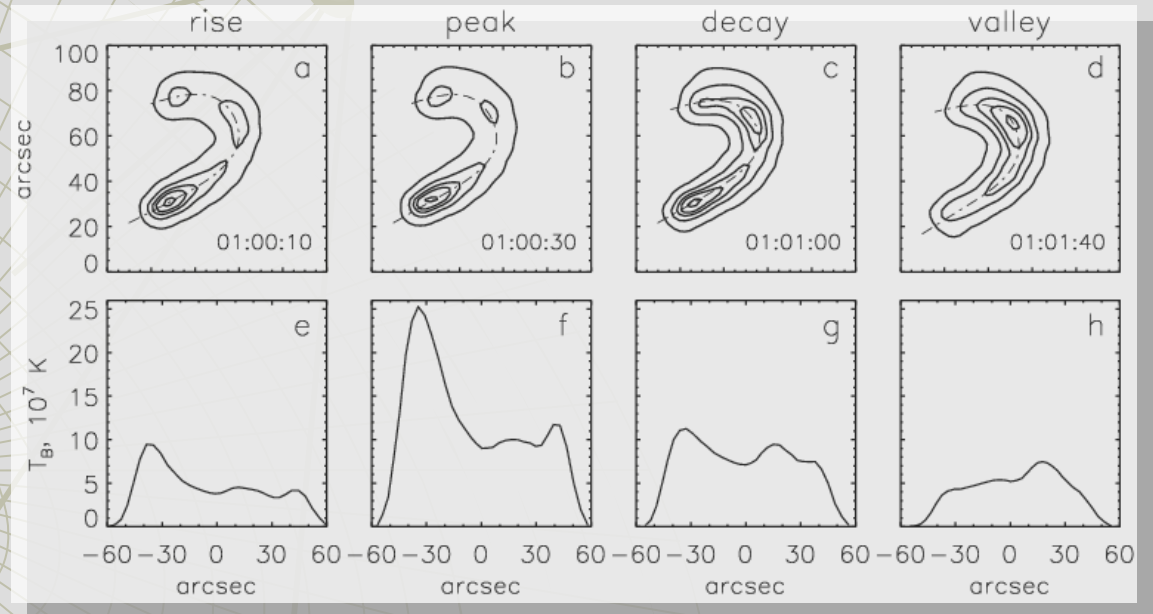
Models:

- Isotropic injection in the center and near the footpoints of a magnetic trap.
- Anisotropic injection along and across magnetic field in the center and near the footpoints of a magnetic trap.
- Isotropic and anisotropic injection along and across magnetic field when the injection function is homogeneous along the whole loop



No one of the simple models gives a full agreement with the observed properties of the brightness distribution dynamics:

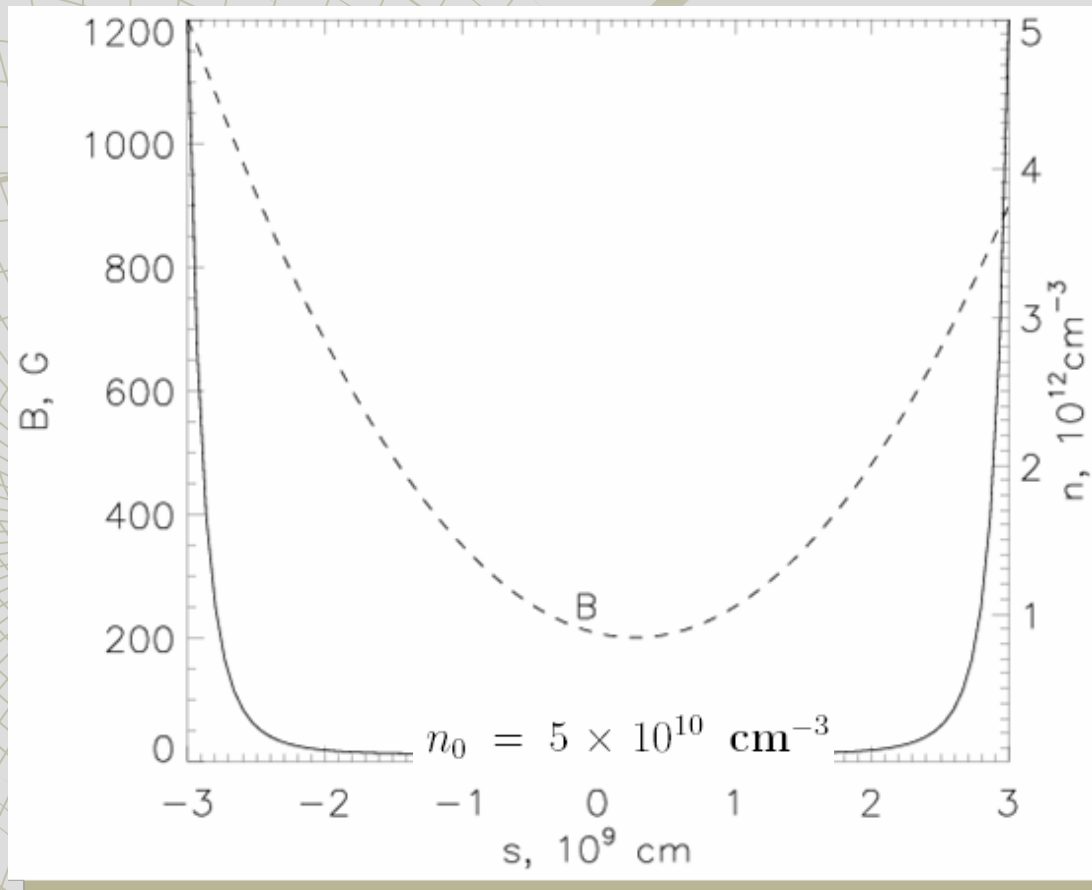
- 1) Assymetry of the distribution on the rise and maximum phase;
- 2) Time delays;
- 3) Type of dynamics



However, we have found a more complicated model which describes the observed properties.

Magnetic field & plasma density distribution along the loop

Magnetic trap is asymmetrical & plasma density is inhomogeneous along the loop

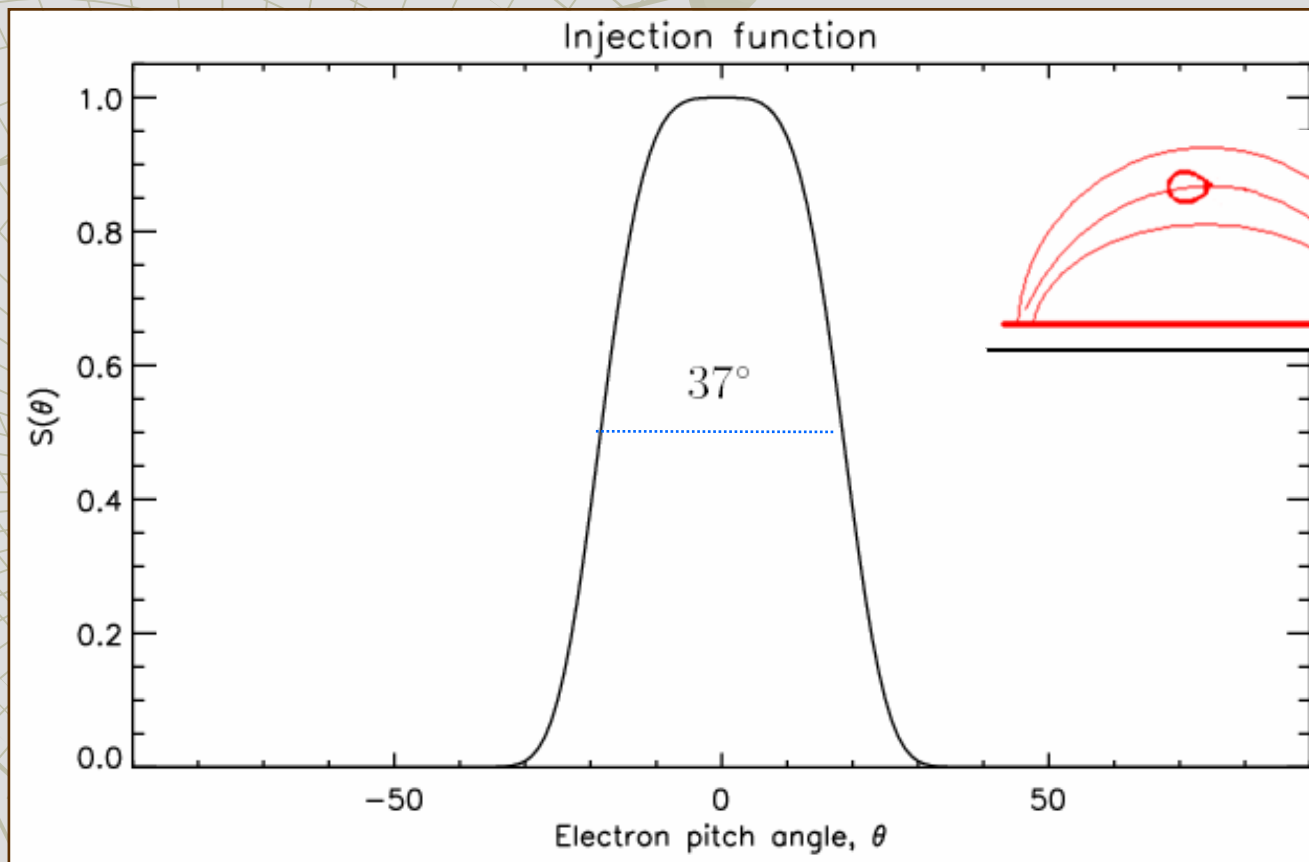


Pitch-angle distribution of injection function

$$S_2(\mu) = \exp[-(\mu - 1)^2 / \mu_0^2] + \varepsilon,$$

where $\varepsilon = 3.4 \times 10^{-4}$

$$\mu_0 = 0.062$$

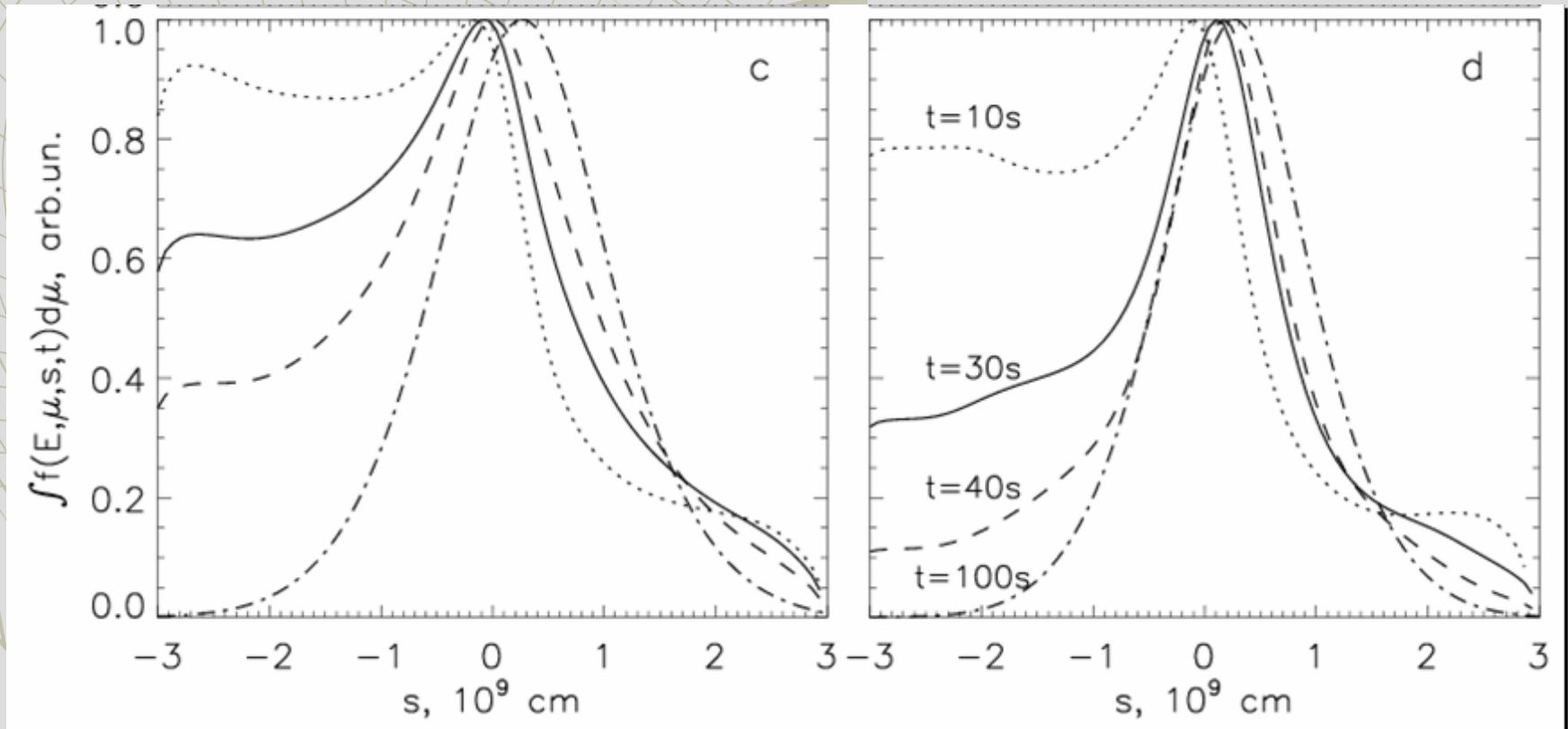


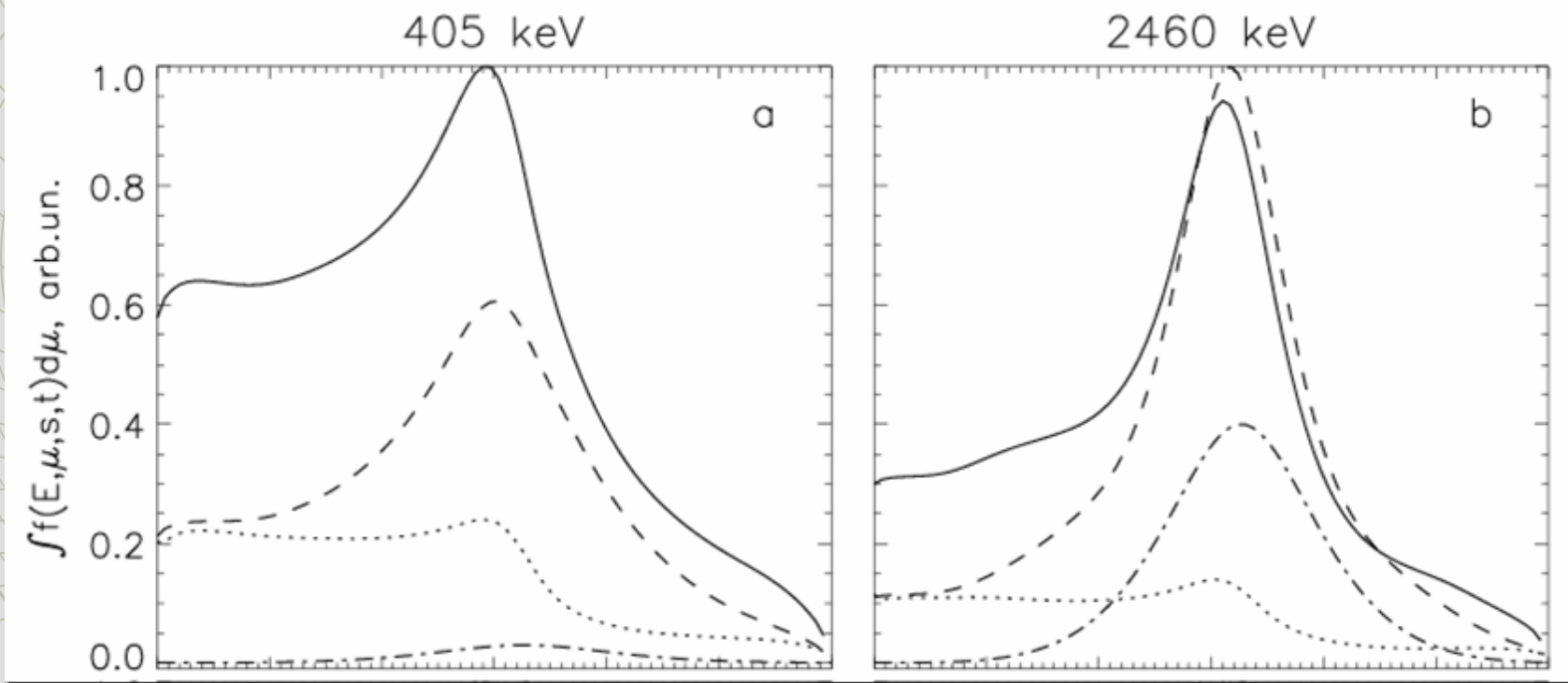
Results of model simulations

Step 1. The time evolutions of electron number density distribution

405 keV

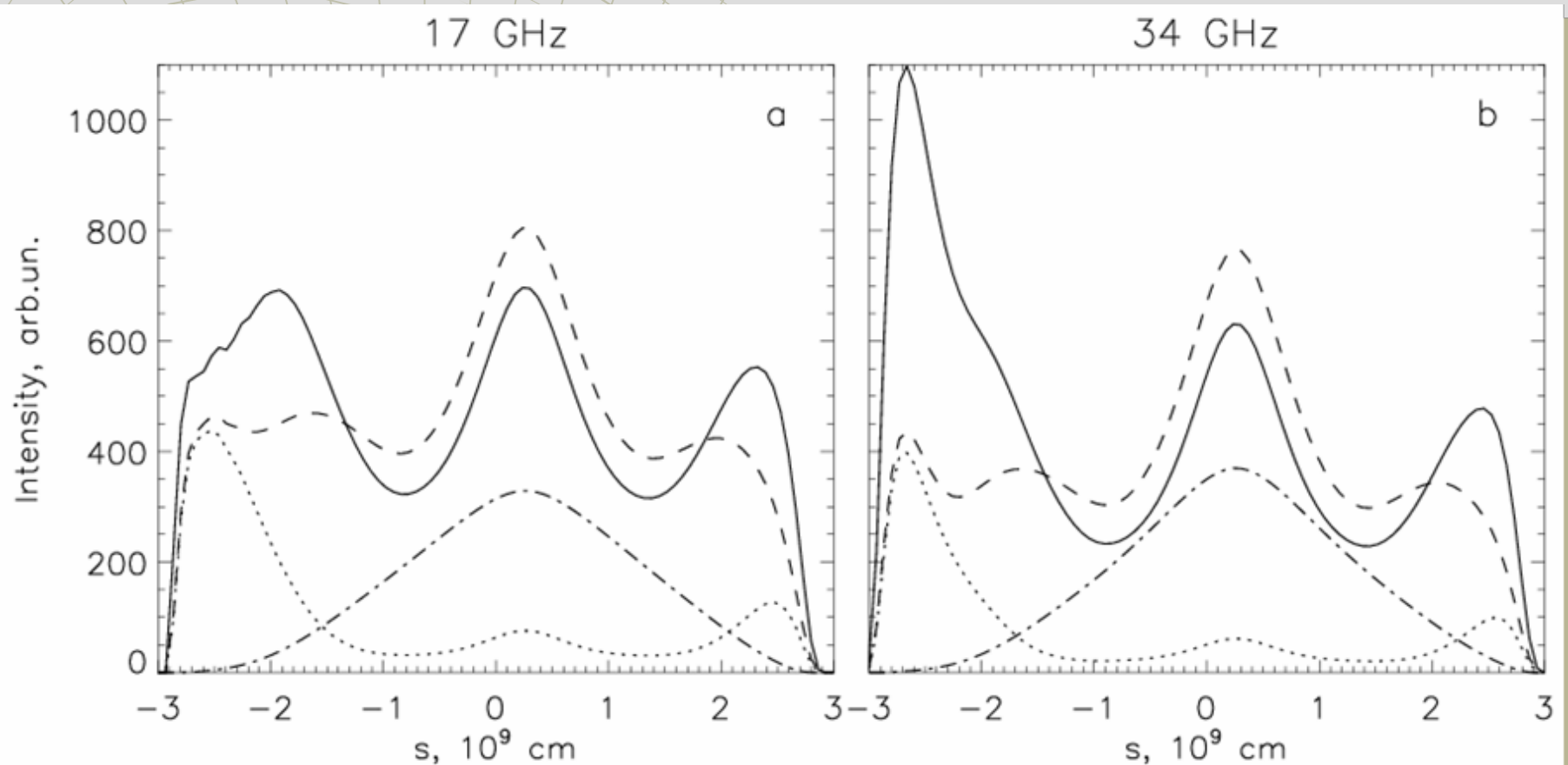
2460 keV





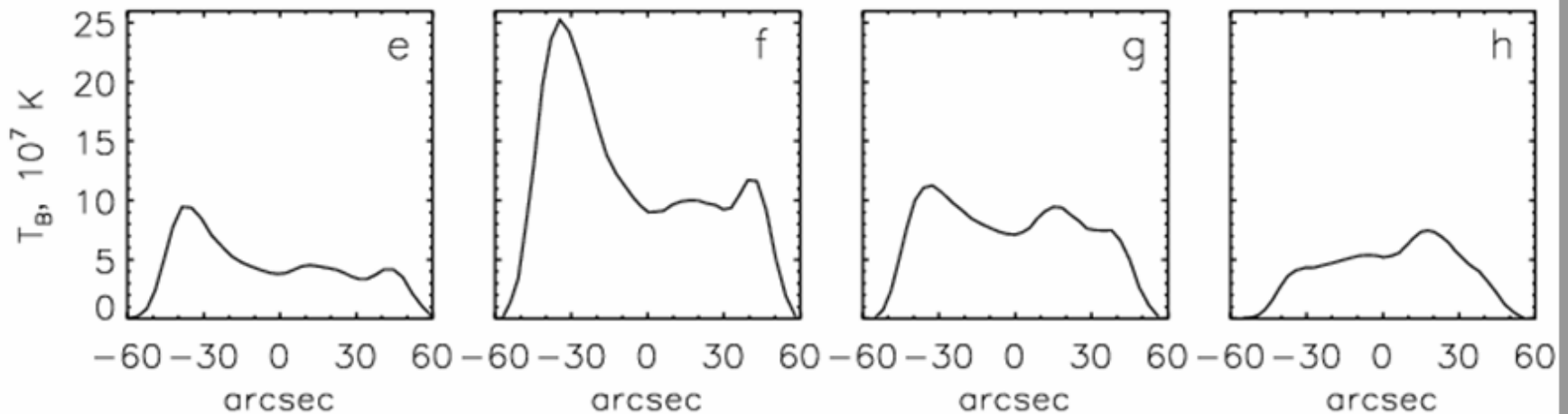
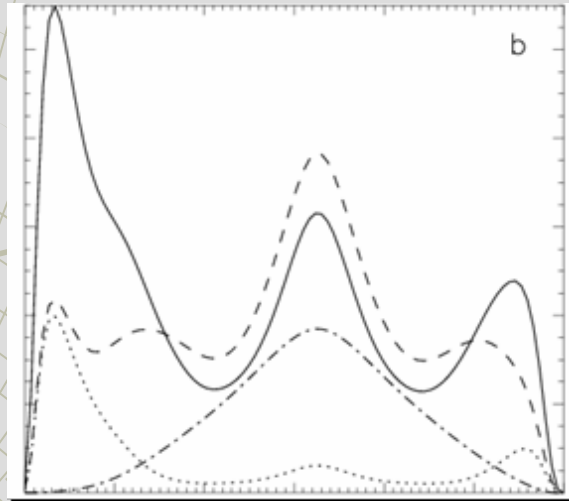
On the decay phase, the number density of electrons with higher energy, 2460 keV decreases much slower than at energy 405 keV.

Step 2. Evolution of gyrosynchrotron emission distribution along the model loop



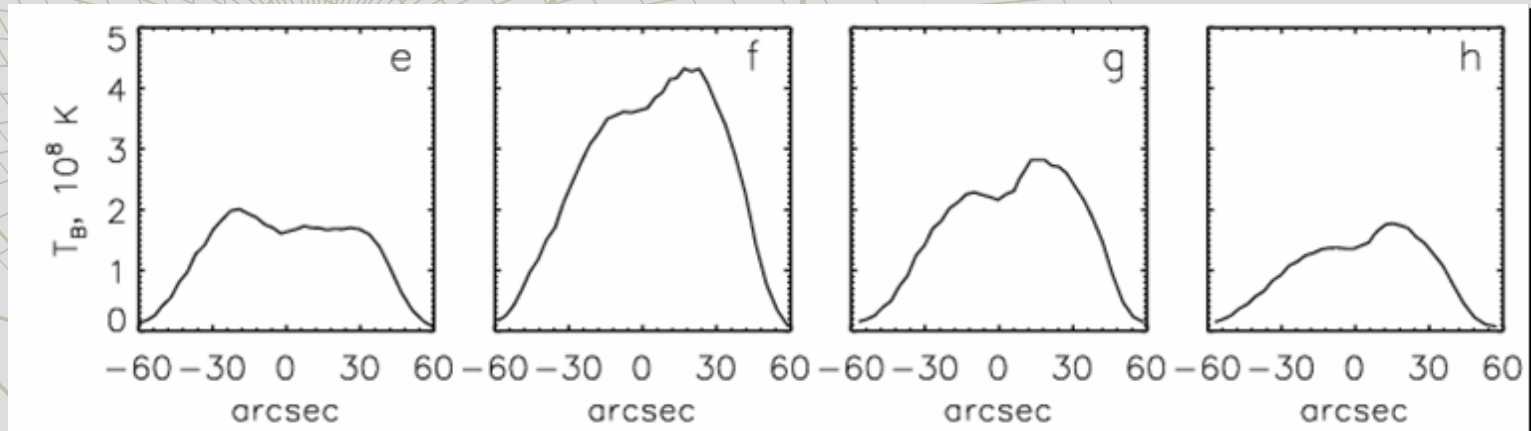
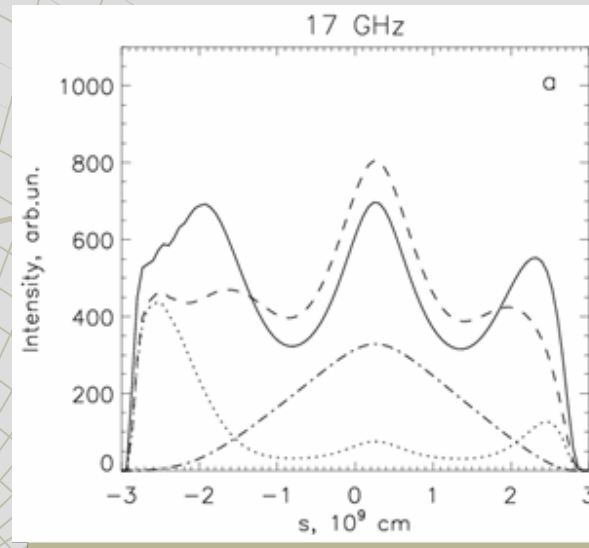
Step 3. A comparison with the observations: similar dynamics

34 GHz



Step 3. A comparison with the observations: similar dynamics

17 GHz



Observational result

We have found the similar dynamics of brightness distribution for all major temporal sub-peaks of the burst:

- ◆ *on the rising phase* of the radio burst the brightness distribution was highly asymmetric, with a strong maximum near the southern footpoint
- ◆ *on the decay phase*, the loop top gradually became most bright

Result of radio diagnostics

Two important properties:

- ★ *The number density of mildly relativistic electrons in the loop top is much higher than near the footpoints during rise, maximum and decay of each major peak*
- ★ *The ratio of the electron number densities in the loop top and a footpoint increases from the maximum to decay phase*

Result of model simulation

Brightness dynamics similar to the observed can be obtained in the model which is characterized by

- ★ *an asymmetric magnetic trap;*
- ★ *a compact source of electrons near the loop center;*
- ★ *the source is non-stationary and long lasting;*
- ★ *the source is injecting high-energy electrons with the pitch-angle distribution mostly directed toward the SFP but also having a very weak isotropic component;*

Conclusion

Conducted analysis of microwave dynamics, diagnostics of physical parameters, and model simulations have brought us to better understanding of such issues as:

- ★ *the location of injection site*
- ★ *pitch-angle distribution of injected electrons*
- ★ *particle transport*

Thank You!

